ACCOUNTS
of chemical research

Plasmonic Antenna Effects on Photochemical Reactions

SHUYAN GAO,[†] KOSEI UENO,[†,‡] AND HIROAKI MISAWA*[,†]

[†]*Research Institute for Electronic Science, Hokkaido University, Sapporo 001-0021, Japan, and* [‡]*PRESTO, Japan Science and Technology Agency, Kawaguchi 332-0012, Japan*

RECEIVED ON AUGUST 18, 2010

CONSPECTUS

Efficient solar energy conversion has been vigorously pursued since the 1970s, but its large-scale implementation hinges on the availability of high-efficiency modules. For maximum efficiency, it is important to absorb most of the incoming radiation, which necessitates both efficient photoexcitation and minimal electron–hole recombination. To date, researchers have primarily focused on the latter difficulty: finding a strategy to effectively separate photoinduced electrons and holes. Very few reports have been devoted to broadband sunlight absorption and photoexcitation. However, the currently available photovoltaic cells, such as amorphous silicon, and even single-crystal silicon and sensitized solar cells, cannot respond to the wide range of the solar spectrum. The photoelectric conversion characteristics of solar cells generally decrease in the infrared wavelength range. Thus, the fraction of the solar spectrum absorbed is relatively poor. In addition, the large mismatch between the diffraction limit of light and the absorption cross-section makes the probability of interactions between photons and cell materials quite low, which greatly limits photoexcitation efficiency. Therefore, there is a pressing need for research aimed at finding conditions that lead to highly efficient photoexcitation over a wide spectrum of sunlight, particularly in the visible to near-infrared wavelengths.

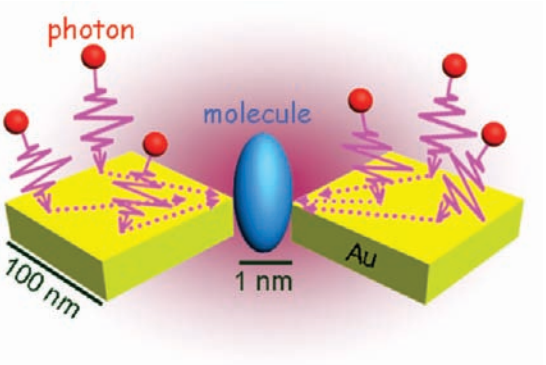

As characterized in the emerging field of plasmonics, metallic nanostructures are endowed with optical antenna effects. These plasmonic antenna effects provide a promising platform for artificially sidestepping the diffraction limit of light and strongly enhancing absorption cross-sections. Moreover, they can efficiently excite photochemical reactions between photons and molecules close to an optical antenna through the local field enhancement. This technology has the potential to induce highly efficient photoexcitation between photons and molecules over a wide spectrum of sunlight, from visible to near-infrared wavelengths. In this Account, we describe our recent work in using metallic nanostructures to assist photochemical reactions for augmenting photoexcitation efficiency.

These studies investigate the optical antenna effects of coupled plasmonic gold nanoblocks, which were fabricated with electron-beam lithography and a lift-off technique to afford high resolution and nanometric accuracy. The two-photon photoluminescence of gold and the resulting nonlinear photopolymerization on gold nanoblocks substantiate the existence of enhanced optical field domains. Local two-photon photochemical reactions due to weak incoherent light sources were identified. The optical antenna effects support the unprecedented realization of (i) direct photocarrier injection from the gold nanorods into TiO_2 and (ii) efficient and stable photocurrent generation in the absence of electron donors from visible (450 nm) to near-infrared (1300 nm) wavelengths.

Introduction

Nanoparticles of noble metals exhibit characteristic bands of optical attenuation at visible and infrared wavelengths due to localized surface plasmons (LSPs).[1] Derived from the study and utilization of such unique optical properties, plasmonics is a flourishing new field in science and technology. Recent years have witnessed a dramatic growth in both the number and the scope of plasmonic applications.[2] Optical antenna effects endow plasmonic nanostructures with the unique ability to break the diffraction limit of light and the possibility of squeezing light into subwavelength volumes to convert optical radiation into

Published on the Web 03/07/2011 www.pubs.acs.org/accounts
10.1021/ar100117w

localized fields with magnitudes of $\sim 10^5$ times the incident energy; that is, field-enhancement effects. Consequently, plasmonic nanostructures will likely improve the mismatch between the small dimensions of nanoscale devices and the length scale associated with optical wavelengths, as well as enhance absorption cross sections. The highly localized fields also result in new interaction mechanisms between light and matter, such as higher-order multipole transitions or momentum-forbidden transitions.[2−4] Since the first successful demonstrations of plasmon-induced photosynthesis[5] and charge separation,[6] scientists have eagerly pursued the study of plasmon-assisted photochemical reactions that perform efficiently from visible to IR/near-infrared (NIR) wavelengths. If such reactions can be achieved, a new class of visible-light-to-NIR-sensitive solar energy converters should follow. The development of such converters is both challenging and attractive, especially with the current demand for greener power generation in which sunlight is efficiently converted to electricity. Therefore, we focused on the development of efficient antenna structures as a way to control light−matter interactions on the nanometer scale in order to increase the efficiency of the photochemical reaction and to develop a method for efficient photocurrent generation with a wide spectral response.

The overall efficiency of plasmon-assisted photochemical reactions is closely related to the absorption cross-section and the consequent probability of interactions between photons and molecules, which depends on the optical antenna effect. The amplitude of the confined plasmon in metallic nanoparticle systems is maximized when the gap is at a minimum (ideally $\ll 10$ nm), but it should be larger than zero considering the influence of quantum-mechanical effects occurring close to the metal surface in very small plasmon gaps.[7] Due to the simplicity, chemical methods remain the choice for many investigators seeking to elaborate plasmonically coupled nanoparticle arrangements. However, random particle locations and spacing make it difficult to accurately tune local resonance frequencies or to define the areas experiencing the largest field enhancements.[8]

In this Account, we highlight our recent work,[9−16] beginning with a presentation of the available gold nanoblocks and selected structural designs constructed with nanometric accuracy using electron-beam lithography (EBL) and a lift-off technique. We then illustrate how the LSPs can be precisely controlled as a function of the structural designs (size, shape, aspect ratio, orientation, and gap width) from visible to NIR spectral range. Next, we demonstrate evidence for gap-dependent field enhancement effects via two-photon photoluminescence (PL) and nonlinear photopolymerization and our exciting experimental observations that nonlinear photochemical reactions can be successfully induced by weak incoherent radiation sources. By increase of the absorption cross-section and boosting of the probability of interactions between photons and molecules due to the optical antenna effect, this inspiring result substantially advances the goal of constructing efficient photoelectronic energy converters for use in plasmonic solar cells that can operate in a wide spectral range encompassing visible and NIR wavelengths. Finally, we describe what work remains to be done to realize this goal.

Preparation Strategy

Our research concept is to construct patterned arrays of gold nanoblocks with nanometric accuracy to take advantage of the optical antenna effects originating from their coupled configurations and thus generate efficient photochemical reactions with a wide spectral response. This concept is, however, exclusively dependent on our ability to structure metals in a controlled and reproducible manner at sub-10-nm resolutions. One of the most common high-resolution nanopatterning techniques is EBL, which is a powerful means to fabricate metallic nanostructures on a solid substrate, and actually the method has already been used for plasmonic research.[17−19] As illustrated in Figure 1, our preparation strategy is a direct application of EBL followed by a lift-off technique for the purpose of creating nanoengineered arrays of coupled plasmonic gold nanoblocks with high resolution. By rationally adjusting the size, shape, aspect ratio (*R*, the ratio of the length to the width of the nanoblocks), orientation, and nanogap width, we could fabricate arrays of nanoblock pairs and rectangular nanoblocks, checkerboard patterns, and orderly nanorod arrays, as shown in Figure 2.[9−16]

Optical Properties

LSP frequencies scale not only with absolute dimensions, but also with *R*; thus, spectral tuning of the LSP via structural tailoring is crucial for obtaining a plasmonic response at the required wavelength.[1,3,17] We use arrays of $34 \times 300 \times 40$ nm^3 rectangular gold nanoblocks to illustrate the convenient tuning of LSPs made possible by the precise control of the size and *R* of the nanoblocks during fabrication. The interval between each structure was set at 200 nm to prevent near-field interactions between neighboring

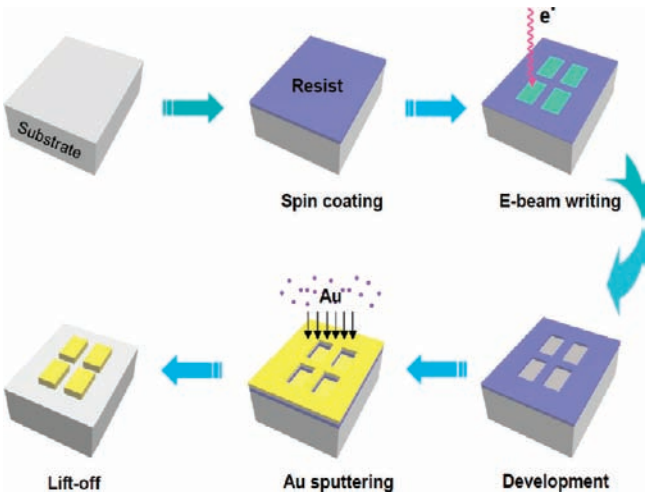

FIGURE 1. Schematic diagram of the direct application of EBL followed by the lift-off technique for the fabrication of coupled plasmonic gold nanoblocks.

nanoblocks although far-field interactions based on lattice effects can be observed as in previous reports.[20,21] The unpolarized extinction spectra of gold nanoblocks with various R values are shown in Figure 3A. For $R = 1$, each extinction spectrum exhibits a single peak near the 700 nm wavelength. For higher R values, a distinct branching into two bands can be seen in the visible region from 620 to 550 nm and in the IR/NIR region from 930 to 1500 nm. These are the transverse plasmonic (TP) and longitudinal (LP) bands, respectively. Note that the longitudinal peaks are red-shifted, whereas the transverse peaks are blue-shifted, with the shift magnitude strongly dependent on R. This behavior is in agreement with Gans's prediction[22] and previously obtained experimental results for gold nanorods.[23] In addition, the measured spectra indicate that the TP and LP modes of identical and parallel nanoblock arrays can be selectively excited by controlling the linear polarization orientation of the incident light, as depicted in Figure 3B,C. These observations demonstrate that the ordered arrays of nanoblocks with nanometric accuracy can facilitate spectral tuning of the TP and LP bands, achieve control over the LSPs from the visible to the NIR regions, and serve as an ideal platform for the study and application of their optical properties unhindered by various side effects resulting from fluctuations in shape, size, orientation, and density.[9−11]

Characterization of the Near-Field Enhancement Effect at the Nanogap Position

In addition to their tunable optical properties and wide spectral range, patterned gold nanoblocks are expected to exhibit spatially enhanced optical fields. A number of studies have been reported on two-photon excited PL from gold and its application in observing enhanced electric fields.[24,25] Taking checkerboard patterns of nanoblocks as a model system, we verified and evaluated the plasmonic near-field enhancement based on the dependence of gold PL intensity on the designed nanogap width. Figure 4A shows an SEM image of a sample containing nine checkerboard gold clusters with different nanogap widths. Figure 4B shows the gold PL intensity map of the same structure. At the irradiation power used, only a weak PL was detected at nanogap widths exceeding 14 nm. The gold PL intensity increased sharply when the nanogaps were less than 14 nm. No PL could be detected from smooth gold films, even at an increased irradiation power.

Figure 4C compares the PL spectra from ensembles of nanoblock pairs with 0 nm-wide gap (i) and relatively wide gaps of 56 nm (ii). The PL yields were much stronger in i than ii, indicating the importance of nanoblock coupling. The dependence of PL intensity on the nanogap width (Figure 4D) exhibits a sharp maximum at a nanogap width of several nanometers, indicating that the integral intensity of the optical near field at the surface and inside the gold nanoblocks is strongest at this separation. This observation is in good agreement with the prediction that maximizing the PL yield for resonant optical antennae requires the gaps between the particles to be as small as only a few nanometers.[26] The PL intensity exhibited a square-law dependence on the excitation power, as shown by the inset in Figure 4D, suggesting that nonlinear two-photon absorption (TPA) is the dominant mechanism of photoexcitation at the wavelength of 800 nm, an interpretation that was further confirmed by theoretical calculations using finite-difference time-domain (FDTD) modeling of linear Maxwell equations. Figure 4E shows the field-intensity enhancement factor at the wavelength of 800 nm for a structure with a 1.5-nm nanogap. The enhancement factor is largest in the nanogap region, where it reaches about 10^4, a much higher value than would be achievable with isolated nanoparticles or on rough surfaces.[27,28] The key feature of our structures is an intense near field existing in nanogaps of only a few nanometers between the nanoblocks. The degree of localization of these modes and the corresponding PL intensity can be tuned by adjusting the nanogap width, which in turn substantiates the field-enhancement effects and accuracy of nanofabrication.[12]

Although our observations clearly demonstrate that near-field enhancement can be engineered via structural tailoring

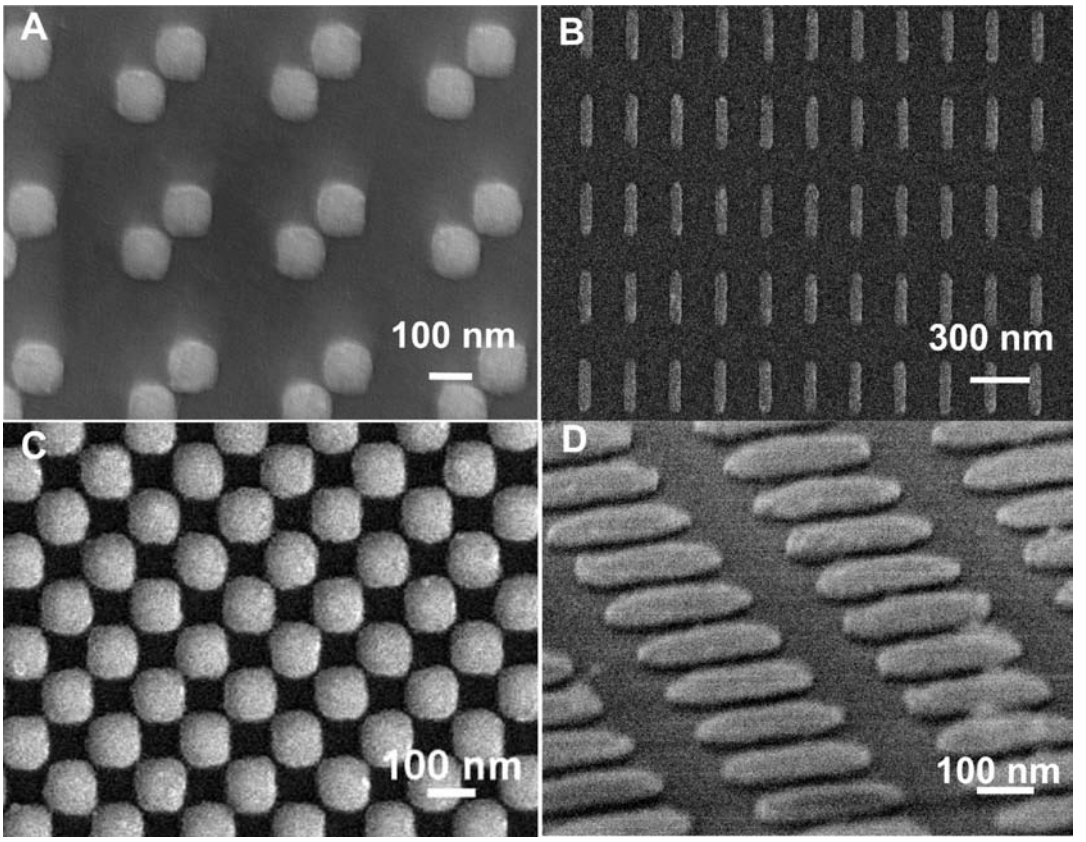

FIGURE 2. Scanning electron microscopy (SEM) images of the representative patterned gold nanoblocks: (A) arrays of nanoblock pairs; (B) arrays of gold nanorods; and (C) a checkerboard cluster of nanoblocks separated by nanogaps. Panel D is an SEM image of the gold nanorods on TiO_2 tilted at an angle of 75°. Adapted from Misawa et al.[10,16,21]

of nanoparticle geometry and mutual arrangement, a high-resolution experimental assessment of the near-field effects and their spatial distribution was also necessary. Near-field imaging techniques are a most attractive way to elucidate spatial structures of optical near field in the neighborhood of the metal nanostructures.[29,30] As another approach, we recently realized near-field diagnostics simply by embedding plasmonic nanostructures in a photoresist that was then exposed to the near field, creating permanent snapshots for postexposure inspection by high-resolution SEM. In the present study, a negative-type photoresist (SU-8, Microchem Co.) was selected as the photosensitive sample.[31] The SEM images in Figure 5A(a,c) show pairs of gold nanoblocks with regions of polymerized SU-8 resulting from exposure to a femtosecond Ti:sapphire laser with a pulse length of 120 fs, a central wavelength of 800 nm, and a repetition rate of 80 MHz. When the laser beam was polarized linearly along the axis of the pairs (Figure 5A(a)), LP modes localized in the nanogaps induced significant local photopolymerization after a short exposure of 0.01 s. When the laser beam was polarized perpendicular to the axis of the pairs, TP modes with fields concentrated at the left and right tips of the nanoblocks were excited, inducing photopolymerization in the corresponding regions (Figure 5A(c)).[32] Photopolymerization in the nanogaps remained negligible even after a much longer exposure of 100 s. The field-intensity patterns calculated by FDTD correspond closely to the experimental photopolymerization patterns, as shown in Figure 5A(b,d). For the LP mode, the field was localized predominantly in the nanogaps, with a local enhancement factor of up to 6.3×10^3. For the TP mode, a maximum enhancement of up to 85-fold was reached at the left and right corners of the nanoblocks. The lower field-enhancement factor for the TP modes explains why longer exposure was needed.

Axial and lateral modifications of the polymerized structures after prolonged exposure are compared in Figure 5B. One would expect that by designing different patterns, the propagation of polymerization can be guided beyond the illuminated area. The approximate sizes and total volumes of photopolymerized SU-8 regions at different laser powers and exposure times were estimated, and the exponential growth of the polymerized volume with exposure time is

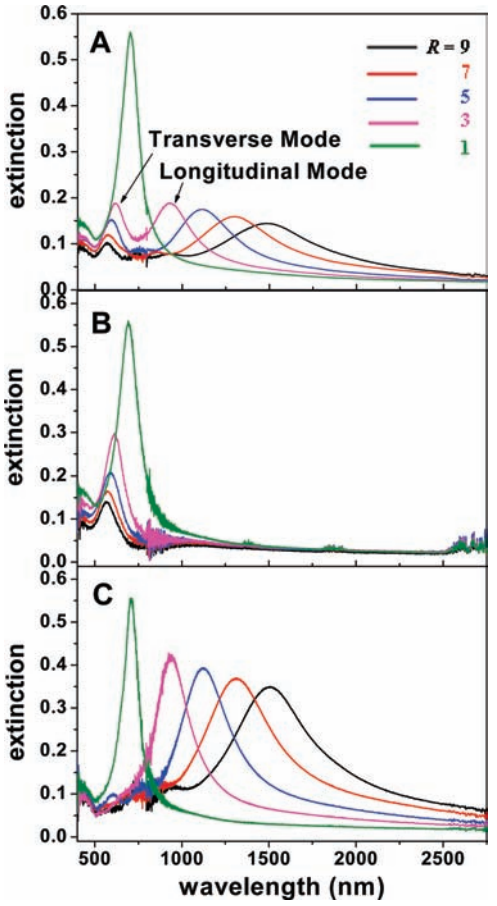

FIGURE 3. Extinction spectra of gold nanoblocks with different *R* values under nonpolarized irradiation (A) and polarized irradiations (B, C). Panels B and C employ light polarized perpendicular and parallel, respectively, to the elongation direction of the rectangular blocks. Each is 40 × 360 nm in lateral dimensions, and blocks are spaced 200 nm apart. Adapted from Misawa et al.[18]

evident. This growth reflects the nonlinear response via multiphoton absorption. Field enhancement in the nanogap and its penetration into gold nanoparticles may have produced this nonlinear photopolymerization. The spatial patterns of the photopolymerized material, in turn, resemble the near-field patterns that induced photopolymerization. Thus, such near-field contact photography can be successfully applied for high-resolution spatial mapping of the enhanced near-field regions, and the maps obtained are consistent with theoretically calculated near-field patterns.[13−15]

Nonlinear Photochemical Reaction Initiated by an Incoherent Light Source

The second law of photochemistry states that each absorbed photon activates one molecule for a photochemical reaction. An exception to this rule is nonlinear absorption, in which more than one photon is consumed. It is commonly accepted that excitation of substantial nonlinear absorption requires a coherent laser source. To our excitement, we have observed that in the surrounding high-plasmonic-field regions, TPA can efficiently trigger a nonlinear photochemical reaction and induce gap-dependent two-photon polymerization (TPP) under irradiation by incoherent radiation sources.[13]

For plasmonic field enhancement, we prepared gold nanoblocks measuring 120 × 120 × 40 nm^3, arranged in a checkerboard pattern with 6-nm nanogaps at their nearest corners. Such structures possess LSPs for which the enhanced near field is predominantly localized in the nanogaps. We first confirmed that, as before, two-photon polymerization proceeded by irradiation using a monochromatic continuous wave laser (785 nm) as an excitation source at the nanogap and determined the total exposure doses inducing polymerization. In the experiment under irradiation by an incoherent radiation source, we used a halogen lamp spectrally filtered to the wavelength range of 600−1000 nm. Figure 6A shows an SEM image of the structure after 3 h of exposure to the source, polarized linearly along the arrow, and the postprocessing of SU-8. As shown here, lines of nanogaps parallel to this direction were filled with polymerized SU-8, whereas along the perpendicular direction the nanogaps were empty. This arrangement indicates that the dominant collective LP mode was excited only in the chains of nanoblocks oriented along the polarization direction. In contrast, exposure to an unpolarized source, which excites LP modes along both chain directions, led to polymerization in all nanogaps, as shown in Figure 6B. It is well documented that SU-8 is optically insensitive at visible and NIR wavelengths.[33] Photopolymerization resulting from exposure in this spectral region is commonly ascribed to TPP.[31,34] The field-intensity patterns obtained from FDTD calculations (Figure 5A(b,d)) corresponded closely to the experimental photopolymerization patterns, indicating that, at the central wavelength of the continuous-wave source (800 nm), LP modes are strongly localized in the nanogaps with high local intensity. Thus, nonlinear absorption and photopolymerization of SU-8 in the nanogaps is the most likely explanation for our observations.

Although the two-photon sensitivity of photopolymers has already been exploited for the near-field imaging of nanoparticle plasmon modes under laser excitation,[31,34] our work is crucially different from previous studies in that it demonstrates that TPA can be induced under exposure to a continuous-wave, incoherent radiation source by increasing the cross-section for TPA in the high-plasmonic-field regions. This result illustrates that the TPA theory proposed in 1931[35] can be verified experimentally without a laser excitation.

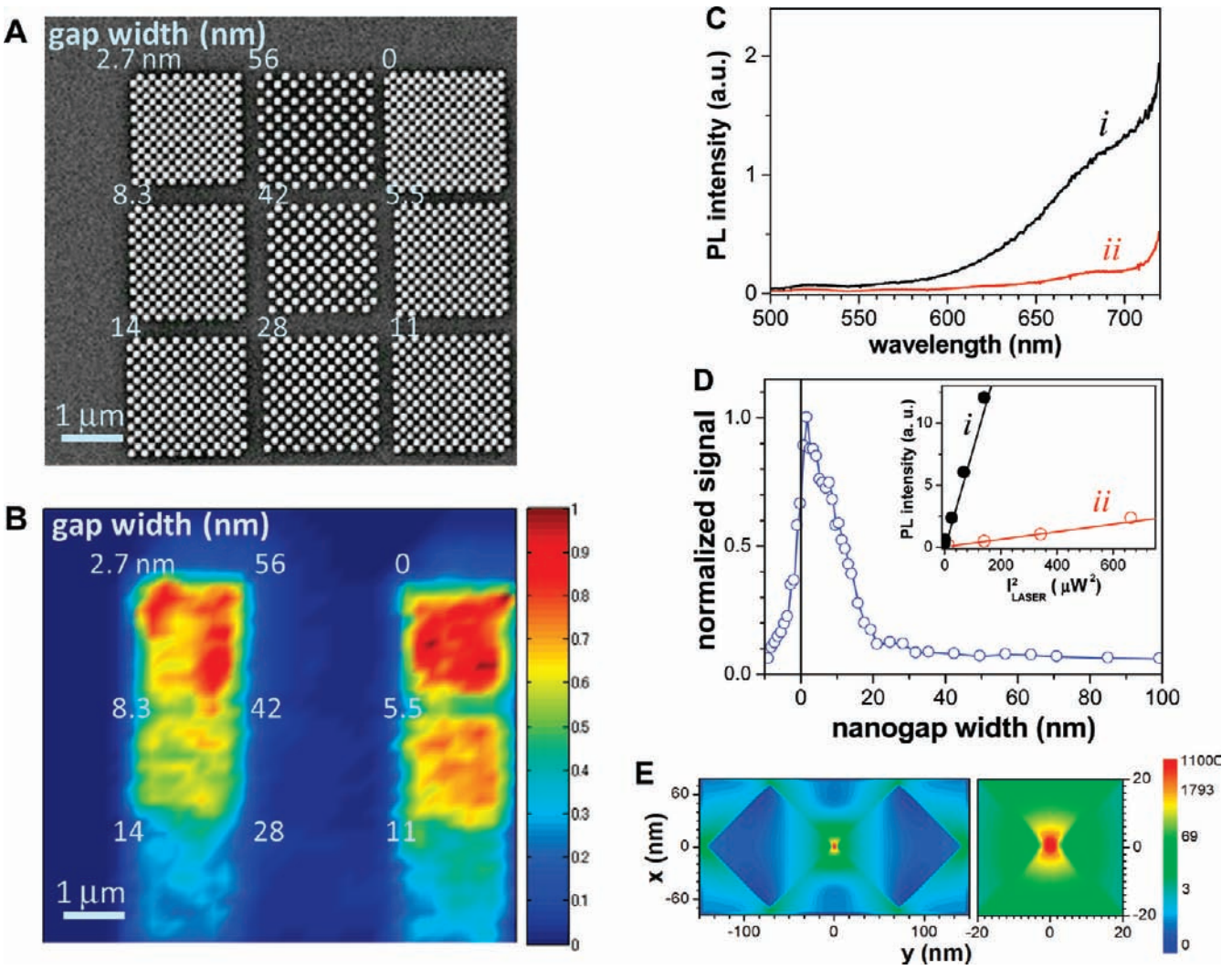

FIGURE 4. (A) SEM image of the $8 \times 8\ \mu m^2$ area of the sample containing nine checkerboard nanoblock clusters. The numbers indicate the different nanogap widths (in nanometers). (B) Spatial map of the PL intensity (linear scale) from the same sample. (C) PL spectra from paired nanoblocks with 0 nm wide gap (i) and a relatively wide gap of 56 nm (ii). (D) Nanogap-width dependence of the PL intensity. The dependence is normalized to their maximum values. The inset shows the square-law dependence of the PL intensity on the excitation power for nanoblocks with 0 nm wide gap (i) and a relatively wide gap of 56 nm (ii). (E) Calculated spatial map of the optical near-field intensity enhancement factor for a structure with a 1.5 nm nanogap and a wavelength of 800 nm. Adapted from Misawa et al.[16]

Plasmon-Assisted Photocurrent Generation

In view of the outstanding features of the arrays of coupled plasmonic nanoblocks, such as facile tunability of LP resonances from the visible to NIR spectral range and enhanced optical fields, we hoped to achieve plasmonic photoelectric conversion from the visible to NIR wavelength range by using electrodes in which gold nanorods are elaborately arrayed on the surface of single-crystal TiO_2. The SEM image is shown in Figure 2D. The nanorods' extinction spectra (Figure 7A) depict a broad LSP around the wavelengths of 650 and 1000 nm. The TP (650 nm; red curve) and LP (1000 nm; blue curve) can be selectively excited by controlling the orientation of the linear polarization of the incident light. Measurements of the photocurrent density versus irradiation time (the $I-t$ curve) showed that the observed photocurrent was quite stable for more than 200 h. The incident-photon-to-photocurrent efficiency (IPCE) values of the photocurrent, 6.3% and 8.4%, correspond to the LSPs in the T-mode at 650 nm and in the L-mode at 1000 nm, respectively (Figure 7B). Note that no photocurrent was observed at the TiO_2 single crystal without gold nanorods under irradiation of light with a wavelength of 450 nm or longer, which demonstrates that electron injection from the gold nanorods to the TiO_2 single-crystal substrate was induced by LSP excitation. In other words, photocurrent generation is associated with LSP excitation. In addition,

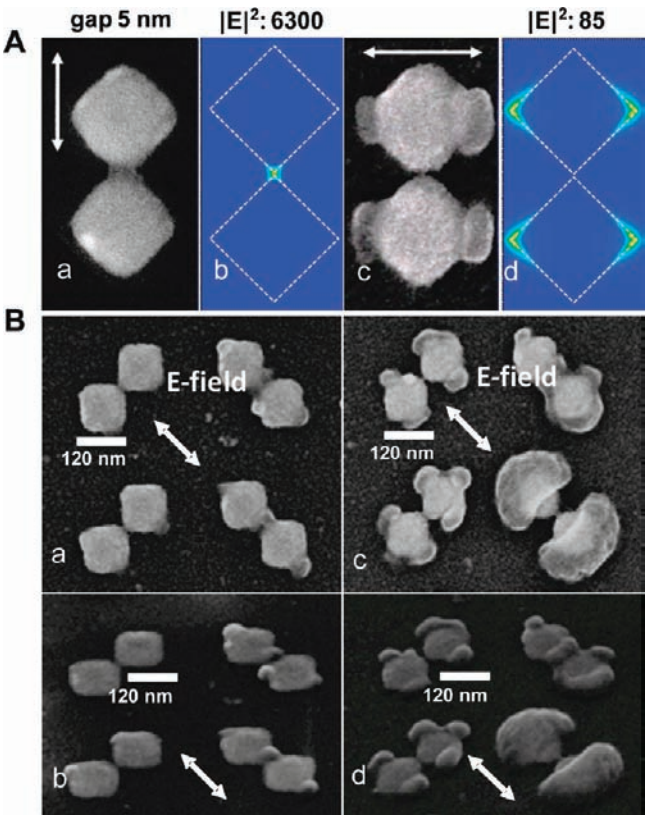

FIGURE 5. (A) (a, c) SEM images of nanoblock pairs after 0.01 and 100 s of exposure to a laser beam polarized linearly along the long axis of the pair and (b, d) theoretical near-field patterns calculated by FDTD for the excitation conditions of the samples shown in panels a and c. (B) SEM images of photopolymerized SU-8 on top of gold nanoblock pairs after 0.01 s (a, b) and 100 s (c, d) of exposure to a laser beam with a power of 2 kW/cm^2 and a peak intensity of 516 MW/cm^2. The nanoblock pairs are the same as those shown in panel A. The inset arrow shows the incident polarization direction. SEM images were obtained from the top (a, c) and from an angle of 45° (b, d). Adapted from Misawa et al.[12,15]

the TiO_2 single crystal with gold nanorods enabled photocurrent generation by irradiation with IR light at longer wavelengths, from 800 to 1300 nm, as well as by irradiation in the visible range.

Figure 7C shows the relationship between the internal quantum efficiency (IQE) value and the wavelength of incident monochromatic light and clearly demonstrates that the quantum efficiencies near the LSPs of the T-mode and L-mode depended on the wavelength and that there were local maximum values for each mode. The IQE, determined by correcting the IPCE for the absorption efficiency of gold nanorods, reflects the absorbed-photon-to-electron conversion efficiency of gold nanorods.[36] Transmission/scattering losses exist at the maximum wavelengths of the plasmon absorption and red shift the long wavelength peak in the IQE curve. This is quite different from general photoelectrochemical systems, where the IQE does not depend on the wavelength of the absorption spectrum of the sensitizer driving the photoelectron transfer.[36] This result suggests that photoinduced electron transfer from gold nanorods to TiO_2 resulting from the excitation of LSPs is nonlinearly induced by both optical antenna effects and electromagnetic field-enhancement effects. Note that such an efficient photocurrent can be observed without including specific electron donors. This observation, together with the fact that the photocurrent was stable for more than 200 h without the addition of donors, suggests that water molecules may act as donors that inject electrons into the d-band holes with the assistance of LSP excitation.

A proposed mechanism of the anodic photocurrent generation is illustrated in Figure 7D.[16] When the LSPs are

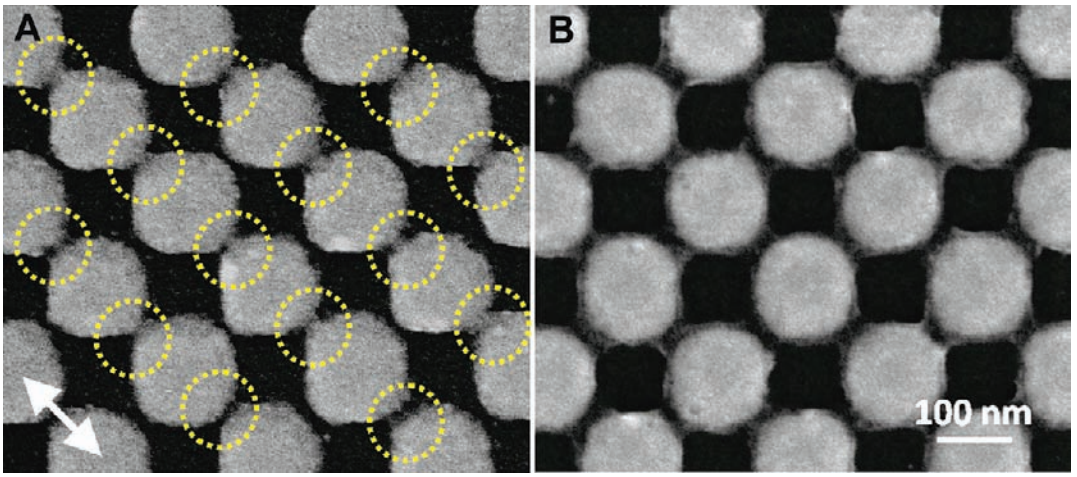

FIGURE 6. (A) SEM image of the structure after 3 h of exposure to an incoherent light source polarized linearly in the direction indicated by the arrow. The polymerized regions are shown in dashed circles. Panel B is the same as panel A after exposure to an unpolarized source. Adapted from Misawa et al.[15]

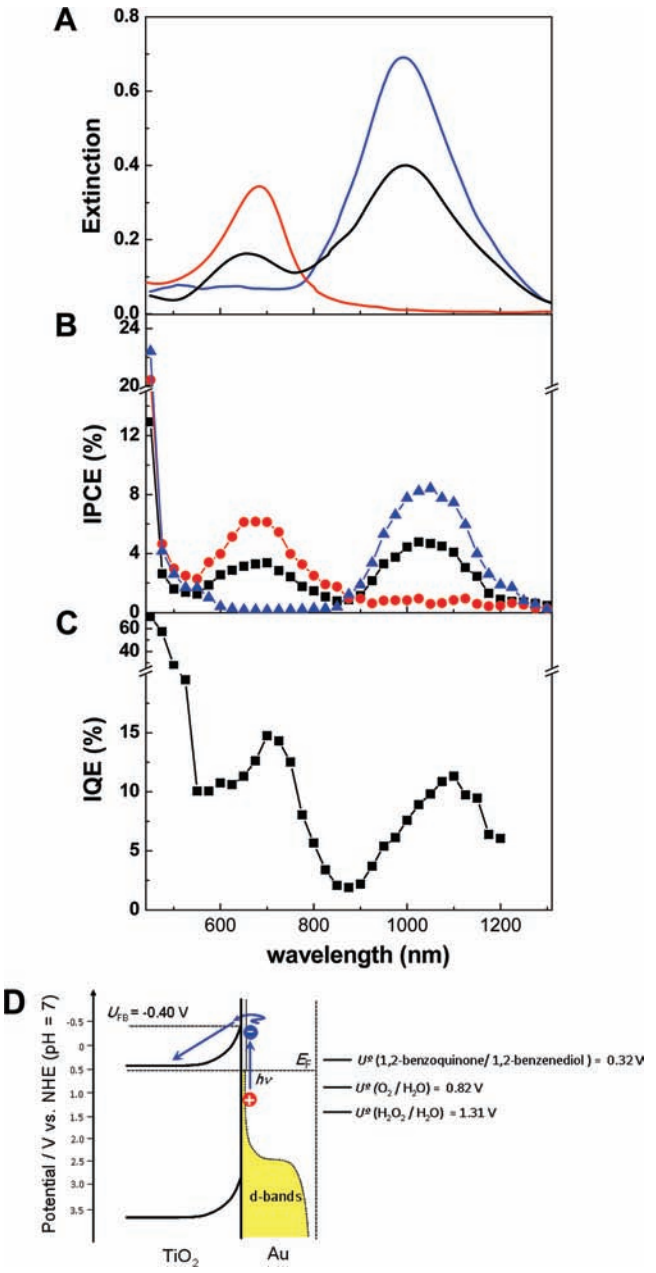

FIGURE 7. (A) Extinction spectra of the gold nanorods: black, under irradiation with unpolarized light; red and blue, T-mode and L-mode under irradiation with linearly polarized light. (B) IPCEs at each wavelength with monochromatic light. Black, red, and blue curves represent the same conditions as in panel A. (C) IQE obtained by standardizing IPCE. (D) Energy diagram of electron excitation based on between-band transfer. Adapted from Misawa et al.[21]

excited by light of wavelengths shorter than 700 nm, an interband transition from the d-bands to the sp-conduction band may be promoted, and pairs of excited electrons and electron holes should form around the interface between the gold nanorods and TiO_2, whereas the holes should be trapped at the TiO_2 surface states.[37] The density of states in the gold d-bands decreases at around 1.8 eV from the Fermi level.[38] Therefore, the probability of an interband transition from d-band to sp-conduction band excited by the 700−1300 nm wavelengths is very low. However, the intense optical near field locally enhanced by plasmonic effects at the edges of the gold nanorods may assist in the electron excitation of gold even at NIR wavelengths, resulting in successful electron transfer from gold nanorods to the conduction band of TiO_2. Actually, some researchers succeeded in observing anodic photocurrents based on the plasmon-assisted electron transfer from gold to TiO_2 electrode and measuring the electron transfer dynamics using transient absorption spectroscopy.[6,39,40] A multiple electron-transfer process via the oxidation of water molecules can contribute to photocurrent generation if electron transfer via tunneling is induced at an energy barrier lower than the flat band of TiO_2, an effect resulting from locally enhanced intense optical near fields or the flat-band potential of the gold nanostructures deposited on an n-TiO_2 wafer inducing a positive shift, as reported previously.[41]

The present plasmon-assisted photocurrent generation system is a great improvement over the previously reported photovoltaic cell.[42,43] First, the plasmon system enables photoelectric conversion for a very wide range of wavelengths from visible to NIR light. Because it can use light with wavelengths from 800 to 1300 nm, which is the spectrum window for biological systems, it has the potential for use as a solar cell embedded in living tissue. Furthermore, larger photocurrent generation is achieved by the optical−electric field enhanced by the LSPs. It is expected, therefore, that a highly efficient photoelectric conversion system can be developed by designing gold nanorods that exhibit larger optical field-enhancement effects and effective generation of LSPs. In addition, this system could potentially be used as a new solar cell that allows multiple-electron photolysis of water molecules.[21]

Conclusions and Outlook

Our results demonstrate that plasmonic nanostructures with optical antenna effects provide a promising platform to promote photochemical reactions with high efficiency, perform nonlinear photochemical reactions using weak incoherent radiation sources, and induce photocurrent generation from light in the visible to NIR range, thereby contributing to the realization of a low-carbon-use society.

Conceptually, optical antenna effects in plasmonic nanostructures are likely to be useful in any type of photocurrent generation system where light concentration and localization are beneficial. Despite our recent achievements in this area, a number of challenges remain. (1) One should

keep in mind the ohmic damping and intrinsic radiation losses of the LSP. Our previous work focused on planar arrays, but many other structural designs can benefit from the increased light confinement and field enhancement. For example, a semiconductor photovoltaic light absorber can be two-dimensionally embedded inside the plasmonic cavity such that light is concentrated in the nanogap based on optical antenna effects; here, the formerly lost energy is ingeniously trapped by the semiconductor, the ohmic damping and radiation losses are substantially reduced, and thus photocurrent will be efficiently generated. A three-dimensionally ordered closely spaced design of metallic nanostructures (stacked and uneven type) is also a promising alternative given the formation of hierarchical nanogaps. In stacked-type metallic nanostructures, the field enhancement exists not only at the horizontal gaps, but also at the vertical ones. In addition, in uneven metallic nanostructures, the field enhancement can be tremendously magnified at the sharp gaps (the tips), which is the basis of the well-documented top-down configuration for achieving ideal field enhancement and minimizing radiation losses. (2) A molecule in the vicinity of a nanogap is exposed to a strong electromagnetic field gradient related to the nanometer-sized nanogap space (meaning that the molecular size and the gradient of the electromagnetic field are comparable), such that the selection rule for the molecular excitation could be controlled. This is because the long-wavelength approximation does not apply in this situation. This experimental observation is expected when using nanometer-wide-gap structures. (3) Although it is speculated that smaller particles, with effective dipole moments located closer to the semiconductor layer, and the coupling between plasmons, excitons, and phonons in metal−semiconductor nanostructures (i.e., interface science) comprise a rich field of research, so far, this area of study has received little attention.[44] (4) Advanced analytical techniques are required to fully understand and utilize this technology. The most effective technique currently available is interferometric time-resolved photoemission electron microscopy, which offers a revolutionary methodology for imaging the ultrafast dynamics of coherent fields and excited carriers in nanometer-scale optical and electronic structures. This technique can be employed for the study of LSP dynamics in nanoclusters and for the direct spatial observation of the hot-electron lifetimes in metallic nanostructures.[45] Time-resolved transient-absorption spectroscopy also shows promise for elucidating the ultrafast electron transfer process from gold to the conduction band of TiO_2 electrode. Together with a near-field optical microscopy technique with a spatial resolution of less than 10 nm and simulation by FDTD, the above techniques could dynamically characterize the field distribution and its dependence on structural designs and further determine the optimal conditions for achieving strong coupling between photons and molecules. This will in turn guide the structural design and facilitate the advantage of using light localization in high-efficiency photochemical reactions and the corresponding photovoltaics, thereby furthering the realization of a low-carbon-use society.

The United Nations declared 2011 as the International Year of Chemistry. Chemistry will certainly continue to make important contributions toward solving the global energy problem. The innovative designs of plasmonic-assisted photochemical reactions show tremendous promise for useful energy-converting applications, and we look forward to their continued development with considerable optimism.

We dedicate this paper to Professor Paul Barbara (senior editor), who passed away on October 31, 2010. The authors are very grateful to our colleagues, Dr. Naoki Murazawa, Dr. Vygantas Mizeikis (currently affiliated with Shizuoka University), Dr. Yoshiaki Nishijima, Dr. Yukie Yokota, and Dr. Toshiyuki Shibuya for their important contributions to this research. This work was supported by funding from the Ministry of Education, Culture, Sports, Science and Technology of Japan, via the KAKENHI Grant-in-Aid for Scientific Research in the Priority Area "Strong Photon-Molecule Coupling Fields" (No. 470 (No. 19049001)), and Grants-in-Aid from Hokkaido Innovation through Nanotechnology Support (HINTS).

BIOGRAPHICAL INFORMATION

Shuyan Gao received her Ph.D. from the Changchun Institute of Applied Chemistry, Chinese Academy of Sciences, in 2006 under the supervision of Professor Hongjie Zhang. From 2007 to 2009, she worked as a JSPS research fellow in Dr. Naoto Koshizaki's laboratory at the National Institute of Advanced Industrial Science and Technology. She is currently a postdoctoral researcher in Professor Hiroaki Misawa's research group at Hokkaido University. She holds a professorship at Henan Normal University. Her research includes plasmon-based optical transducers and construction of unique nanostructures for application in green chemistry.

Kosei Ueno is an associate professor at the Research Institute for Electronic Science at Hokkaido University, Japan. He received his Ph.D. in chemistry from Hokkaido University in 2004. From 2004 to 2006, he worked in Professor Hiroaki Misawa's laboratory as a JSPS research fellow. He became an assistant professor at Hokkaido University in 2006 and was promoted to associate professor in 2008. Since 2007, he has held an additional post as a PRESTO

researcher at the Japan Science & Technology Agency (JST). His current scientific interests are the fabrication and optical characterization of gold nanostructures defined with subnanometer precision and their plasmonic applications, especially in the research field of chemistry.

Hiroaki Misawa is a director and professor at the Research Institute for Electronic Science at Hokkaido University, Japan. He received his Ph.D. in chemistry from the University of Tsukuba in 1984. After postdoctoral positions at the University of Texas (USA) and the University of Tsukuba (Japan) and an assistant professorship at Tsukuba University, he joined the Microphotoconversion project (ERATO) of the Japan Science & Technology Agency (JST). He became an associate professor in the Department of Engineering at the University of Tokushima in 1993 and was promoted to full professor in 1995. He moved to Hokkaido University as full professor in 2003. His current research interests include photochemistry, light−matter interaction, ultrafast processes in materials, photonic crystals, and plasmonics. He has authored more than 200 papers.

FOOTNOTES

*E-mail: misawa@es.hokudai.ac.jp. Phone: +81-11-706-9358. Fax: +81-11-706-9359.

REFERENCES

1 Prodan, E.; Radloff, C.; Halas, N. J.; Nordlander, P. A Hybridization Model for the Plasmon Response of Complex Nanostructures. *Science* **2003**, *302*, 419–422.

2 Schuller, J. A.; Barnard, E. S.; Cai, W.; Jun, Y. C.; White, J. S.; Brongersma, M. L. Plasmonics for Extreme Light Concentration and Manipulation. *Nat. Mater.* **2010**, *9*, 193–204.

3 Tabor, C.; Van Haute, D.; El-Sayed, M. A. Effect of Orientation on Plasmonic Coupling between Gold Nanorods. *ACS Nano* **2009**, *3*, 3670–3678.

4 Gramotnev, D. K.; Bozhevolnyi, S. I. Plasmonics beyond the Diffraction Limit. *Nat. Photonics* **2010**, *4*, 83–91.

5 Jin, R.; Cao, Y.; Mirkin, C. A.; Kelly, K. L.; Schatz, G. C.; Zheng, J. G. Photoinduced Conversion of Silver Nanospheres to Nanoprisms. *Science* **2001**, *294*, 1901–1903.

6 Tian, Y.; Tatsuma, T. Mechanisms and Applications of Plasmon-Induced Charge Separation at TiO_2 Films Loaded with Gold Nanoparticles. *J. Am. Chem. Soc.* **2005**, *127*, 7632–7637.

7 Zuloaga, J.; Prodan, E.; Nordlander, P. Quantum Description of the Plasmon Resonances of a Nanoparticle Dimer. *Nano Lett.* **2009**, *9*, 887–891.

8 Clark, A. W.; Cooper, J. M. Optical Properties of Multiple-Split Nanophotonic Ring Antennae. *Adv. Mater.* **2010**, *22*, 4025–4029.

9 Ueno, K.; Mizeikis, V.; Juodkazis, S.; Sasaki, K.; Misawa, H. Optical Properties of Nanoengineered Gold Blocks. *Opt. Lett.* **2005**, *30*, 2158–2160.

10 Ueno, K.; Juodkazis, S.; Mizeikis, V.; Sasaki, K.; Misawa, H. Spectrally Resolved Atomic-Scale Length Variations of Gold Nanorods. *J. Am. Chem. Soc.* **2006**, *128*, 14226–14427.

11 Ueno, K.; Juodkazis, S.; Mino, M.; Mizeikis, V.; Misawa, H. Spectral Sensitivity of Uniform Arrays of Gold Nanorods to Dielectric Environment. *J. Phys. Chem. C* **2007**, *111*, 4180–4184.

12 Ueno, K.; Juodkazis, S.; Mizeikis, V.; Sasaki, K.; Misawa, H. Clusters of Closely-Spaced Gold Nanoparticles as a Source of Two-Photon Photoluminescence at Visible Wavelengths. *Adv. Mater.* **2008**, *20*, 26–30.

13 Ueno, K.; Juodkazis, S.; Shibuya, T.; Yokota, Y.; Mizeikis, V.; Sasaki, K.; Misawa, H. Nanoparticle Plasmon-Assisted Two-Photon Polymerization Induced by Incoherent Excitation Source. *J. Am. Chem. Soc.* **2008**, *130*, 6928–6929.

14 Ueno, K.; Juodkazis, S.; Shibuya, T.; Mizeikis, V.; Yokota, Y.; Misawa, H. Nanoparticle-Enhanced Photopolymerization. *J. Phys. Chem. C* **2009**, *113*, 11720–11724.

15 Ueno, K.; Takabatake, S.; Nishijima, Y.; Mizeikis, V.; Yokota, Y.; Misawa, H. Nanogap-Assisted Surface Plasmon Nanolithography. *J. Phys. Chem. Lett.* **2010**, *1*, 657–662.

16 Nishijima, Y.; Ueno, K.; Yokota, Y.; Murakoshi, K.; Misawa, H. Plasmon-Assisted Photocurrent Generation from Visible to Near-Infrared Wavelength Using a Au-Nanorods/TiO_2 Electrode. *J. Phys. Chem. Lett.* **2010**, *1*, 2031–2036.

17 Hicks, E. M.; Zou, S.; Schatz, G. C.; Spears, K. G.; Van Duyne, R. P.; Gunnarsson, L.; Rindzevicius, T.; Kasemo, B.; Käll, M. Controlling Plasmon Line Shapes through Diffractive Coupling in Linear Arrays of Cylindrical Nanoparticles Fabricated by Electron Beam Lithography. *Nano Lett.* **2005**, *5*, 1065–1070.

18 Krenn, J. R.; Schider, G.; Rechberger, W.; Lamprecht, B.; Leitner, A.; Aussenegg, F. R.; Weeber, J. C. Design of Multipolar Plasmon Excitations in Silver Nanoparticles. *Appl. Phys. Lett.* **2000**, *77*, 3379–3381.

19 Schider, G.; Krenn, J. R.; Hohenau, A.; Ditlbacher, H.; Leitner, A.; Aussenegg, F. R.; Schaich, W. L.; Puscasu, I.; Monacelli, B.; Boreman, G. Plasmon Dispersion Relation of Au and Ag Nanowires. *Phys. Rev. B* **2003**, *68*, No. 155427.

20 Auguié, B.; Barnes, W. L. Diffractive Coupling in Gold Nanoparticle Arrays and the Effect of Disorder. *Opt. Lett.* **2009**, *34*, 401–403.

21 Pinchuk, A. O.; Schatz, G. C. Nanoparticle Optical Properties: Far- and Near-field Electrodynamic Coupling in a Chain of Silver Spherical Nanoparticles. *Mater. Sci. Eng., B* **2008**, *149*, 251–258.

22 Gans, R. Form of Ultramicroscopic Particles of Silver. *Ann. Phys.* **1915**, *47*, 270–284.

23 El-Sayed, M. A. Some Interesting Properties of Metals Confined in Time and Nanometer Space of Different Shapes. *Acc. Chem. Res.* **2001**, *34*, 257–264.

24 Bouhelier, A.; Bachelot, R.; Lerondel, G.; Kostcheev, S.; Royer, P.; Wiederrecht, G. P. Surface Plasmon Characteristics of Tunable Photoluminescence in Single Gold Nanorods. *Phys. Rev. Lett.* **2005**, *95*, No. 267405.

25 Imura, K.; Nagahara, T.; Okamoto, H. Near-Field Two-Photon-Induced Photoluminescence from Single Gold Nanorods and Imaging of Plasmon Modes. *J. Phys. Chem. B* **2005**, *109*, 13214–13220.

26 Mühlschlegel, P.; Eisler, H. J.; Martin, O. J. F.; Hecht, B.; Pohl, D. W. Resonant Optical Antennas. *Science* **2005**, *308*, 1607–1609.

27 Wang, H.; Brandl, D. W.; Nordlander, P.; Halas, N. J. Plasmonic Nanostructures: Artificial Molecules. *Acc. Chem. Res.* **2007**, *40*, 53–62.

28 Biesso, A.; Qian, W.; Huang, X.; El-Sayed, M. A. Gold Nanoparticles Surface Plasmon Field Effects on the Proton Pump Process of the Bacteriorhodopsin Photosynthesis. *J. Am. Chem. Soc.* **2009**, *131*, 2442–2443.

29 Imura, K.; Okamoto, H.; Hossain, M. K.; Kitajima, M. Visualization of Localized Intense Optical Fields in Single Gold-Nanoparticle Assemblies and Ultrasensitive Raman Active Sites. *Nano Lett.* **2006**, *6*, 2173–2176.

30 Palomba, S.; Novotny, L. Near-Field Imaging with a Localized Nonlinear Light Source. *Nano Lett.* **2009**, *9*, 3801–3804.

31 Sundaramurthy, A.; Schuck, P. J.; Conley, N. R.; Fromm, D. P.; Kino, G. S.; Moerner, W. E. Toward Nanometer-Scale Optical Photolithography: Utilizing the Near-Field of Bowtie Optical Nanoantennas. *Nano Lett.* **2006**, *6*, 355–360.

32 Ibn El Ahrach, H.; Bachelot, R.; Vial, A.; Lérondel, G.; Plain, J.; Royer, P.; Soppera, O. Spectral Degeneracy Breaking of the Plasmon Resonance of Single Metal Nanoparticles by Nanoscale Near-Field Photopolymerization. *Phys. Rev. Lett.* **2007**, *98*, No. 107402.

33 Witzgall, G.; Vrijen, R.; Yablonovitch, E.; Doan, V.; Schwartz, B. J. Single-Shot Two-Photon Exposure of Commercial Photoresist for the Production of Three-Dimensional Structures. *Opt. Lett.* **1998**, *23*, 1745–1747.

34 Hubert, C.; Rumyantseva, A.; Lerondel, G.; Grand, J.; Kostcheev, S.; Billot, L.; Vial, A.; Bachelot, R.; Royer, P.; Chang, S. H.; Gray, S. K.; Wiederrecht, G. P.; Schatz, G. C. Near-field Photochemical Imaging of Noble Metal Nanostructures. *Nano Lett.* **2005**, *5*, 615–619.

35 Göppert-Mayer, Über, M. Elementarakte mit zwei Quantensprüngen. *Ann. Phys.* **1931**, *401*, 273–294.

36 McFarland, E. W.; Tang, J. A Photovoltaic Device Structure Based on Internal Electron Emission. *Nauture* **2003**, *421*, 616–618.

37 Micic, O. I.; Zhang, Y. N.; Cromack, K. R.; Trifunac, A. D.; Thurnauer, M. C. Trapped Holes on Titania Colloids Studied by Electron Paramagnetic Resonance. *J. Phys. Chem.* **1993**, *97*, 7277–7283.

38 Christensen, N. E. High-Energy Band Structure of Gold. *Phys. Rev. B* **1976**, *13*, 2698–2701.

39 Yu, K.; Tian, Y.; Tatsuma, T. Size Effects of Gold Nanoparticles on Plasmon-Induced Photocurrents of Gold-TiO_2 Nanocomposites. *Phys. Chem. Chem. Phys.* **2006**, *8*, 5417–5420.

40 Furube, A.; Du, L.; Hara, K.; Katoh, R.; Tachiya, M. Ultrafast Plasmon-Induced Electron Transfer from Gold Nanodots into TiO_2 Nanoparticles. *J. Am. Chem. Soc.* **2007**, *129*, 14852–14853.

41 Nakato, Y.; Tsubomura, H. Structures and Functions of Thin Metal Layers on Semiconductor Electrodes. *J. Photochem.* **1985**, *29*, 257–286.

42 Cao, Y. B.; Zhang, J.; Wang, M.; Li, R.; Wang, P.; Zakeeruddin, S. M.; Grätzel, M. High-Performance Dye-Sensitized Solar Cells Based on Solvent-Free Electrolytes Produced from Eutectic Melts. *Nat. Mater.* **2008**, *7*, 626–630.

43 Grätzel, M. A. Photoelectrochemical Cells. *Nature* **2001**, *414*, 338–344.

44 Atwater, H. A.; Polman, A. Plasmonics for Improved Photovoltaic Devices. *Nat. Mater.* **2010**, *9*, 205–213.

45 Kubo, A.; Onda, K.; Petek, H.; Sun, Z.; Jung, Y. S.; Kim, H. K. Femtosecond Imaging of Surface Plasmon Dynamics in a Nanostructured Silver Film. *Nano Lett.* **2005**, *5*, 1123–1127.